



HAL
open science

Silicon Vertical Multijunction Cell for Thermophotovoltaic Conversion

Daniel Chemisana, Oriol Teixidó, Rodolphe Vaillon

► **To cite this version:**

Daniel Chemisana, Oriol Teixidó, Rodolphe Vaillon. Silicon Vertical Multijunction Cell for Thermophotovoltaic Conversion. ACS Energy Letters, 2023, 8 (8), pp.3520 - 3525. 10.1021/acseenergylett.3c01168 . hal-04186071

HAL Id: hal-04186071

<https://hal.science/hal-04186071>

Submitted on 23 Aug 2023

HAL is a multi-disciplinary open access archive for the deposit and dissemination of scientific research documents, whether they are published or not. The documents may come from teaching and research institutions in France or abroad, or from public or private research centers.

L'archive ouverte pluridisciplinaire **HAL**, est destinée au dépôt et à la diffusion de documents scientifiques de niveau recherche, publiés ou non, émanant des établissements d'enseignement et de recherche français ou étrangers, des laboratoires publics ou privés.



Distributed under a Creative Commons Attribution 4.0 International License

Silicon Vertical Multijunction Cell for Thermophotovoltaic Conversion

Daniel Chemisana,* Oriol Teixidó, and Rodolphe Vaillon

Cite This: *ACS Energy Lett.* 2023, 8, 3520–3525

Read Online

ACCESS |



Metrics & More

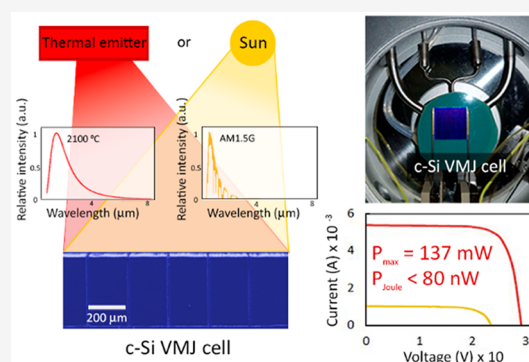


Article Recommendations



Supporting Information

ABSTRACT: A new class of thermophotovoltaic cells converting thermal radiation power into electrical power from sources at very high temperature ($>1800\text{ }^{\circ}\text{C}$) is currently emerging. Like concentrating solar cells, these cells are subject to resistive losses due to high current densities. Hence, tandem cells with horizontally stacked junctions have been recently developed and have achieved record pairwise efficiencies and electrical power densities. Here, we employ alternatively a silicon vertical multijunction cell as a means of reducing current density while operating at high voltage. Both under 1-Sun illumination and that of a thermal source at $2100\text{ }^{\circ}\text{C}$, the cell kept at $25\text{ }^{\circ}\text{C}$ exhibits open-circuit voltages above 25 V and short-circuit currents below 6 mA . With a series resistance below a few milliohms, Joule losses are negligible. The cell receiving $2.01\text{ W}/\text{cm}^2$ and absorbing $1.24\text{ W}/\text{cm}^2$ generates an electrical power density of $0.14\text{ W}/\text{cm}^2$, leading to a pairwise efficiency of only 11.4% because of substantial out-of-band absorption. With photonic engineering of the emitter ensuring no out-of-band emission, this efficiency could reach 52.9% under the same illumination conditions. The cell could also be used under bifacial conditions, which would double the electrical power. However, due to the heat generated in the cell, its temperature can exceed $25\text{ }^{\circ}\text{C}$. Advantageously, a moderate temperature coefficient of the electrical power of $(-0.309 \pm 0.005)\%/^{\circ}\text{C}$ is measured under 1-Sun illumination and it becomes much smaller, $(-0.18 \pm 0.01)\%/^{\circ}\text{C}$, in thermophotovoltaic conditions. These results suggest reopening the path of research aimed at optimizing the design and fabrication of vertical multijunction cells for thermophotovoltaic conversion.



Thermophotovoltaic (TPV) cells allow the conversion of thermal energy into electricity through the photovoltaic effect.^{1,2} Until recently, record-breaking pairwise efficiency TPV cells were made of indium gallium arsenide (InGaAs) operating with an emitter temperature around $1000\text{--}1200\text{ }^{\circ}\text{C}$.^{3–7} Low out-of-band absorption, realized either by reflecting^{5,6} or transmitting^{7,8} as much as possible of the photons with insufficient energy to generate electron–hole pairs, is the means by which efficiencies of 30% or more were achieved. More recently, a pairwise efficiency of 38.8% was reached with an InGaAs cell and a higher emitter temperature than before ($1850\text{ }^{\circ}\text{C}$).⁹ In this work, it is clearly explained that at higher emitter temperature, sub-bandgap absorption is less critical, but high charge collection efficiency is required. The results also show that beyond a current density threshold ($8.7\text{ A}/\text{cm}^2$ passed at emitter temperatures above $1850\text{ }^{\circ}\text{C}$), despite a very low series resistance ($6.5\text{ m}\Omega\text{ cm}^2$), Joule losses affect the efficiency.

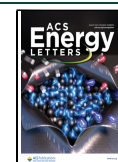
It turns out that a new class of TPV cells is emerging to enable the conversion of thermal radiation from emitters at temperatures above around $1800\text{ }^{\circ}\text{C}$. This evolution accompanies the development of thermophotovoltaic batteries,

where thermal energy is stored at ultrahigh temperature.^{10–13} As the temperature of the thermal source increases, it is logical to use semiconductor materials with a bandgap larger than 1 eV . Silicon is an obvious option that was chosen in the 1980s by Swanson. Remarkably, because of an efficient reflection of out-of-band photons, a pairwise efficiency of 29% was achieved with a $2000\text{ }^{\circ}\text{C}$ blackbody source. Silicon has come back to the forefront very recently,¹⁴ but with an emitter temperature not high enough ($\sim 1715\text{ }^{\circ}\text{C}$) to exhibit series resistance losses caused by high current densities. Logically, as for high concentration solar cells, a solution to mitigate losses by the Joule effect was to design and fabricate cells with multiple junctions. By pursuing this path, tandem cells^{9,15,16} demonstrated high performance in both efficiency and electrical power density. A record efficiency of 41.1% was achieved by a

Received: June 12, 2023

Accepted: July 20, 2023

Published: July 27, 2023



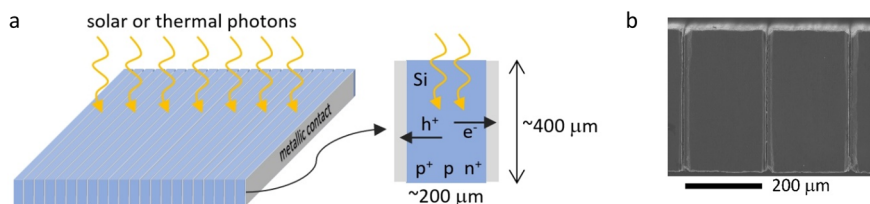


Figure 1. (a) Schematic of a Si vertical multijunction cell. The directions of photon and charge transport are orthogonal. (b) Scanning electron microscopy image of a section of the Si VMJ cell characterized in this work. The alternating vertical layers of silicon and metal are visible in each figure.

1.4 eV GaAs/1.2 eV InGaAs dual-junction cell coupled with an emitter operating at 2400 °C. A record power density of 5.65 W/cm² was measured with a 0.84 eV GaInPAs/0.75 eV InGaAs cell illuminated by a thermal source at 1900 °C. Tandem cells are less prone to series resistance losses but may still be limited by these losses above a certain current density.^{15,16}

Here, we experimentally investigate the alternative option of silicon vertical multijunction (VMJ) cells. Proposed in 1970 as a new type of solar cell,¹⁷ the VMJ structure has attracted attention as a solution to counter resistive losses under ultrahigh concentration conditions. A typical VMJ cell is schematically shown in Figure 1a. It is illuminated from the edge so that photon absorption is vertical while charge transport is horizontal. The cell is free of front and back contacts. This virtually eliminates the shadowing, lateral resistance, and metallic grid resistance losses that are found in conventional cells. A large number of junctions (typically a few dozen per centimeter width) are connected in series so that the cell operates at low current and high voltage. The last two points explain the much lower sensitivity to Joule losses under an extreme solar radiation flux. There are reports of a photoconductivity effect in the lightly doped bulk regions, which leads to a decrease in series resistance at very high illumination.^{18,19} Another advantage, often overlooked, is the lower sensitivity to temperature,²⁰ most probably explained by operation at high voltage.²¹ The main advantages of VMJ cells envisioned for concentrated photovoltaics have been translated into advantageous predictions for thermophotovoltaic conversion,^{22,23} but they have not yet been evaluated experimentally.

A commercial Si VMJ cell is used in the present work. Each of the 50 vertical junctions in series is around 200 μm wide and 400 μm thick, separated by thin silver contacts (Figure 1b). The area of the cell is almost 1 cm² (0.997 × 0.975 cm²). Thus, values provided for current (A) and power (W) can easily be translated into current and power densities (A/cm² and W/cm², respectively). No modifications are made to the cell, and its performance is tested as is. Figure 2 shows the external quantum efficiency (EQE) at 25 °C (a) and the current–voltage curves under 1-Sun illumination (see Experimental Methods) as a function of cell temperature from 25 to 105 °C (b). Since the cell consists of a series of junctions, all of them must be illuminated. Each small vertical junction receives light on an area that is 200 μm wide and 0.975 cm long. Then it makes sense that the spectral response is lower than 1.5%. Indeed, the EQE shown in Figure 2a is fully consistent with the measured short-circuit current shown in Figure 2b. The order of magnitude of the short-circuit current density, less than 0.5 mA/cm², is much less than that of standard silicon cells (~40 mA/cm² under 1-Sun illumination²⁴), as expected by design.

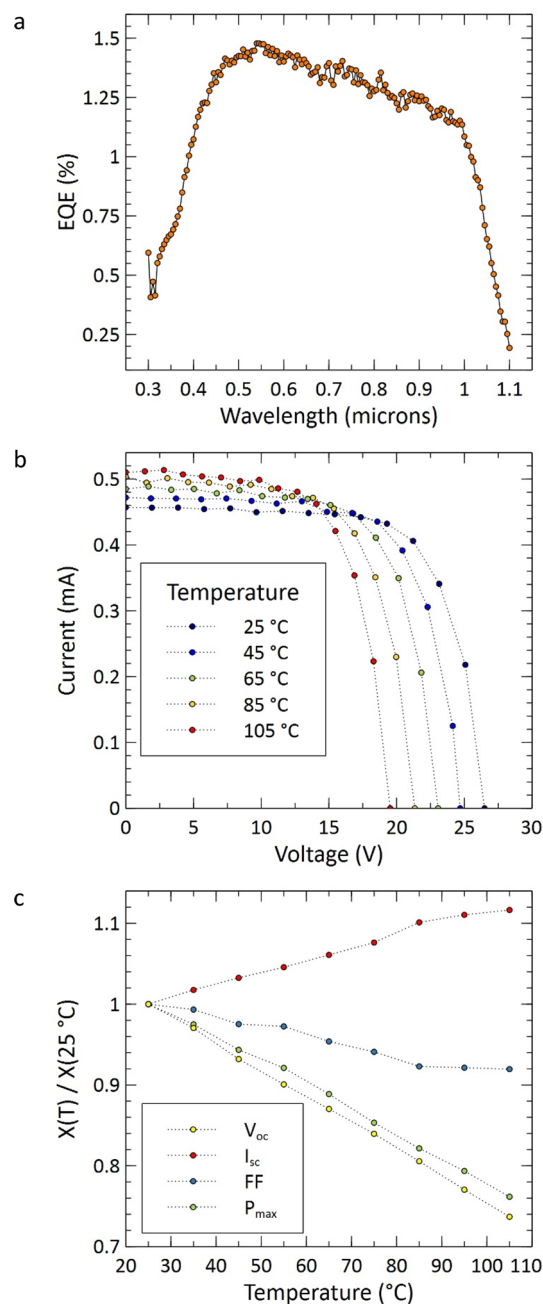


Figure 2. (a) External quantum efficiency of the Si VMJ cell at 25 °C. (b) Current vs voltage for the Si VMJ cell under 1-Sun illumination as a function of cell temperature. (c) Figures of merit (short-circuit current I_{sc} , open-circuit voltage V_{oc} , fill factor FF, and electrical power at the maximum power point P_{max}) as a function of cell temperature, normalized by their value at 25 °C.

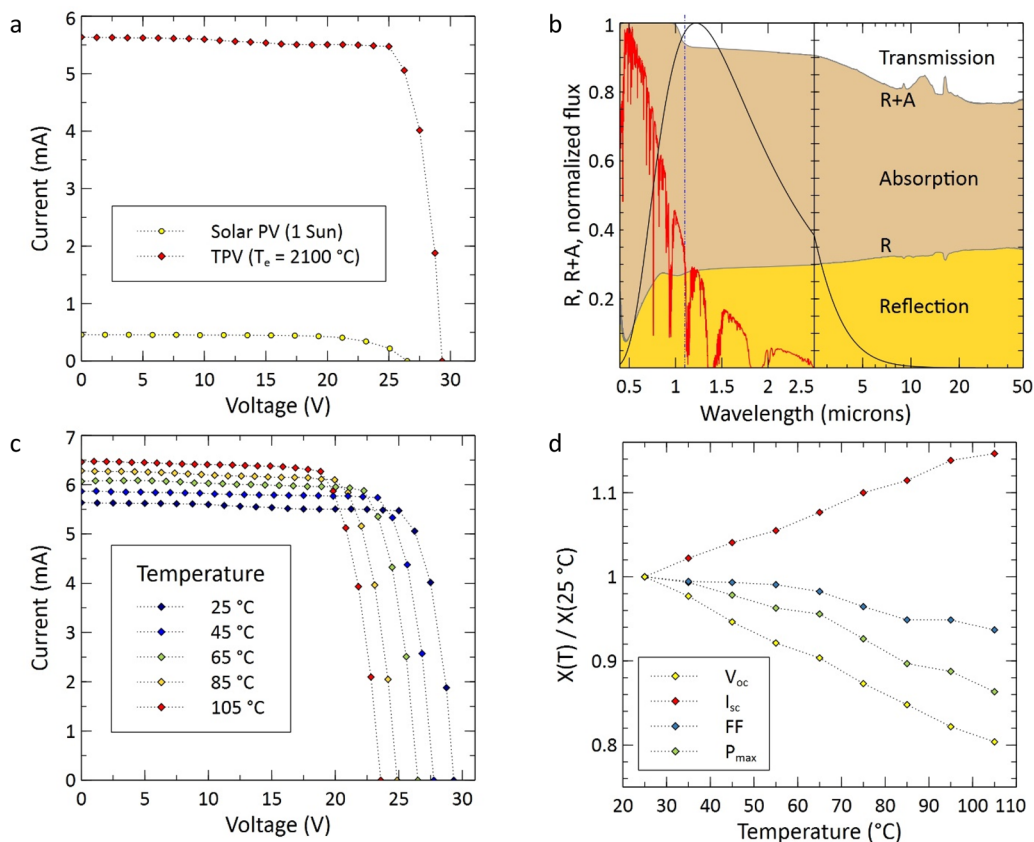


Figure 3. (a) Current vs voltage for the Si VMJ cell at 25 °C under 1-Sun illumination or that of a thermal radiation emitter at 2100 °C (incident radiation power of 1.95 W). (b) Reflectance and sum of reflectance and transmittance of the VJM cell in the spectral range [0.4–50] μm , showing the distribution of reflection, absorption, and transmission of incident radiation by the cell. The normalized spectral flux of global AM1.5 solar irradiation and that of a blackbody at 2100 °C are superimposed. (c) Current vs voltage for the Si VMJ cell under a thermal radiation emitter at 2100 °C (incident radiation power of 1.95 W) as a function of cell temperature. (d) Corresponding figures of merit (short-circuit current I_{sc} , open-circuit voltage V_{oc} , fill factor FF, and electrical power at the maximum power point P_{max}) as a function of cell temperature, normalized by their value at 25 °C.

An EQE can be estimated for a subcell (see Figure S2 in the Supporting Information), with a maximum value close to 74%, as well as the short-circuit current density of a subcell ($\sim 23 \text{ mA}/\text{cm}^2$). In contrast, the open-circuit voltage is much higher than that of a standard silicon cell and reaches 26.5 V at 25 °C. The efficiency of the Si VMJ cell under 1-Sun illumination is calculated to be close to 9% (8.94%). These figures of merit have to be taken with caution since the VMJ cell was designed to operate under very high illumination conditions. The series resistance is very moderate ($\sim 0.15 \text{ m}\Omega$), which, together with low currents, is likely to lead to minimal ohmic losses even under higher illumination.

Figure 2b shows the evolution of current–voltage curves as a function of cell temperature from 25 to 105 °C. Variations of the figures of merit with temperature (see Table S1 in the Supporting Information) follow the usual linear trend as shown in Figure 2c. The temperature coefficients of short-circuit current ($(+0.152 \pm 0.006)\%/^{\circ}\text{C}$), fill factor ($(-0.112 \pm 0.008)\%/^{\circ}\text{C}$), open-circuit voltage ($(-0.328 \pm 0.003)\%/^{\circ}\text{C}$), and electrical power ($(-0.309 \pm 0.005)\%/^{\circ}\text{C}$) are better than the best values for industrial standard silicon solar cells²⁵ and slightly lower than the best values for laboratory silicon solar cells reported in ref 26. The open-circuit voltage temperature coefficient and thus that of electrical power are expected to improve under higher illumination.²¹

Figure 3a shows the current–voltage curves of the Si VMJ cell at 25 °C under 1-Sun illumination and under the illumination of a tungsten-halogen lamp at 2100 °C. Even though in the experimental setup (see the Supporting Information) distance separating the lamp and the cell leads to a very small view factor (1.08%, see Experimental Methods), the radiation power/power density ($\sim 1.95 \text{ W}/2.01 \text{ W}/\text{cm}^2$) incident on the cell is (~ 20.1 times) larger than under 1-Sun illumination ($0.1 \text{ W}/\text{cm}^2$). As a result, the short-circuit current is more than ten times larger (5.64 mA) than under solar irradiation (0.46 mA). The open-circuit voltage (29.3 V) is significantly larger as well. The short-circuit current in TPV conditions is not 20.1 times that under solar PV conditions because the spectra of the sources are very different (see Figure 3b). Most of the spectral radiation power coming from the lamp is in the out-of-band (i.e., at wavelengths larger than 1.1 μm) region for silicon. Nevertheless, in the conditions of the TPV experiment, the VMJ cell still receives more in-band radiation power than under 1-Sun illumination, which explains the larger short-circuit current. It is important to note that the Joule losses remain negligible ($< 80 \text{ nW}$) thanks to the low series resistance ($\sim 2.5 \text{ m}\Omega$) and the low current ($\sim 5.6 \text{ mA}$).

Because of photon recycling, conversion efficiency has a different definition in thermophotovoltaics than in solar photovoltaics.^{1,2} Radiation power reflected by the cell is absorbed by the thermal radiation emitter and thus contributes

to lowering the net heat radiation power lost by the emitter. As a consequence, the primary figure of merit evaluating the performance of a thermophotovoltaic device, called pairwise efficiency, is the ratio of generated electrical power to the radiation power absorbed by the cell.¹ Thus, the VMJ cell absorptance needs to be determined from spectroscopy measurements (Experimental Methods). Figure 3b shows the fractions of incident radiation reflected, absorbed, and transmitted by the cell from 0.4 to 50 μm . As the structure of the VMJ cell is different from that of standard cells, without front and back contacts, its optical behavior is unusual. In particular, because of the absence of a back-contact layer covering the cell, transmittance is not zero (approaching 25%) and reflectance is less than 35% in the out-of-band region (at wavelengths larger than 1.1 μm). As a result, OOB absorptance, ranging from 42 to 66%, leads to moderate photon recycling and a pairwise efficiency of only 11.4%. This result is not surprising since the cell was not designed for thermophotovoltaic conversion. Silicon being weakly absorbing in the infrared, OOB absorption is mainly due to the vertical silver contacts and multiple reflection between them. In the present case, spectral selectivity could be improved by preventing emission from the thermal source in the OOB region, or by putting a filter at the front of the cell perfectly reflecting OOB incident radiation back to the emitter. In that case, calculations indicate that the pairwise efficiency would reach 52.9%. With a view factor of 1.08% between the cell and emitter, the cell generates an electrical power (density) of 136.8 mW (140.7 mW/cm²). Approximate calculations predict slightly better electrical performances under higher illuminations (larger view factors, see Table S3 in the Supporting Information).

In the present configuration with imperfect spectral selectivity, since the VMJ cell is not opaque, unless an optical arrangement transfers the transmitted radiation back to the emitter, the transmitted radiation power should be added to the absorbed radiation power at the denominator of the efficiency, leading to a smaller value of the efficiency (10.1%). Thus, it seems that the absence of a back reflector has only disadvantages. However, the cell could be used in a bifacial configuration, i.e., illuminated at both sides,^{7,8} which would double the electrical power.

Figure 3c displays the evolution of current–voltage curves as a function of cell temperature from 25 to 105 °C. Figure 3d shows the normalized variations of the figures of merit with temperature (see also Table S2 in the Supporting Information). The temperature coefficients of short-circuit current ($+0.188 \pm 0.005\%$ /°C), fill factor ($-0.084 \pm 0.009\%$ /°C), open-circuit voltage ($-0.249 \pm 0.004\%$ /°C), and electrical power at the maximum power point ($-0.18 \pm 0.01\%$ /°C) are different from those under 1-Sun illumination. As expected, the temperature coefficient of the open-circuit voltage is lower due to higher illumination. As a result of combined effects, the temperature coefficient of electrical power is 0.58 times that under 1-Sun illumination.

In conclusion, we have highlighted the peculiar behavior of Si vertical multijunction cells from characterizations under solar and thermal radiation sources. The main advantage of these cells, initially developed for operating under ultrahigh solar concentration, is the negligible Joule losses resulting from low currents. Since silicon cells are meant to be paired with high-temperature (>2000 °C) thermal radiation emitters, the thermal load on the cell is likely to result in a cell temperature

in excess of 25 °C. The second advantage is that the VMJ cell is less sensitive to temperature than standard cells. The far from optimal out-of-band absorption by the VMJ Si cell pleads in favor of designing emitters and/or cell front filters for improving spectral selectivity. By doing so, conversion efficiency as high as 52.9% could be reached. It is important to note that the VMJ cell could be used in a bifacial configuration to double the generated electrical power. VMJ cells might also offer a solution to Joule losses in near-field thermophotovoltaic devices. However, in both the far and near fields, it is worth mentioning that germanium VMJ cells would be best suited for emitters with lower temperature. This work reopens the research pathway for designing thermophotovoltaic devices based on VMJ cells.

EXPERIMENTAL METHODS

Characterization of the VMJ Cell under 1-Sun Illumination. The cell characterized in the present work is an MIH VMJ PV cell (ref 5S1010.4) from MH GoPower.²⁷ The current–voltage (I – V) curves were measured in the standard test conditions (incident radiation power of 0.1 W/cm², AM1.5G spectrum, cell at 25 °C) under the illumination of a solar simulator (Oriel) composed of an AAA xenon-arc lamp. The temperature of the cell was controlled by a thermal stage (Linkam). The irradiance was measured with a pyranometer (CMP10 KIPPZONNEN) with an accuracy of 0.1%. This uncertainty was increased to 0.5% considering the inaccuracy in the distance between the cell or the pyranometer and the lens of the solar simulator. All I – V curves were measured using a Keithley source meter. The external quantum efficiency (EQE) of the cell was determined using an Oriel QEPVSI measurement system. To ensure that the 50 series-connected subcells of the VMJ cell are all illuminated without loss of photons from the source, a reflective truncated inverted pyramid optical element with an exit area corresponding to that of the cell was used. This optical element was attached to both the reference calibrated cell and the VMJ cell. Multiple measurements were carried out to quantify the possible uncertainty caused by incorrect positioning of the optical element on the cells. On average, the uncertainty of the EQE measurement was estimated at $\pm 4\%$.

Characterization of the VMJ Cell Illuminated by a Thermal Radiation Emitter. An experimental setup similar to that reported by LaPotin et al.¹⁶ was developed (see Figure S1 in the Supporting Information). A 5 kW halogen-tungsten lamp was used as the thermal radiation source. It was placed at the focus of an electroplated parabolic concentrator in order to obtain a collimated-like beam. The temperature of the lamp was set by regulating the voltage feeding the lamp using a silicon-controlled rectifier (SCR) with high-power regulator. The voltage was regulated by measuring the electrical resistance of the lamp and following the methodology described in ref 28 to correlate the temperature of the emitter and the lamp feeding voltage. The (Linkam) thermal stage was used to control the cell temperature. All elements around the cell were shielded with an aluminum reflective mask in order to prevent excessive heating. A vertical positioning stage supporting the thermal stage was used to adjust the view factor between the lamp and the cell and thus the incident radiation power on the cell. This power was measured with an Ophir broadband power meter covering the spectral range from 0.19 to 11 μm (with an error of $\pm 4\%$).

Cell Imaging and Radiative Properties. A scanning electron microscope (Jeol) was used to obtain images showing the structure of the VMJ cell. Transmittance (T_λ) and reflectance (R_λ) of the cell were measured in the spectral range [0.4–50] μm by using a Bruker Vertex 70 V FTIR spectrometer with 0.2 cm^{-1} spectral resolution. Specular and diffuse components of the reflectance were measured by using an aluminum integrating sphere (PIKE). Absorptance (A_λ) of the cell was calculated from conservation of energy principles ($A_\lambda = 1 - R_\lambda - T_\lambda$).

■ ASSOCIATED CONTENT

Data Availability Statement

The data that support the findings of this study are available from the corresponding author upon reasonable request.

Supporting Information

The Supporting Information is available free of charge at <https://pubs.acs.org/doi/10.1021/acsenergylett.3c01168>.

Figures of merit as a function of cell temperature and temperature coefficients under 1-Sun and TPV illumination conditions, approximate calculations predicting performances of the cell under higher illuminations, schematic of the TPV experimental setup, estimated external quantum efficiency of a subcell, details on the calculation of the pairwise efficiencies (PDF)

■ AUTHOR INFORMATION

Corresponding Author

Daniel Chemisana – Applied Physics Section of the Environmental Science Department, University of Lleida, Lleida 25001, Spain; orcid.org/0000-0002-6887-5204; Email: daniel.chemisana@udl.cat

Authors

Oriol Teixidó – Applied Physics Section of the Environmental Science Department, University of Lleida, Lleida 25001, Spain

Rodolphe Vaillon – IES, Univ Montpellier, CNRS, Montpellier 34095, France; orcid.org/0000-0002-8559-3604

Complete contact information is available at:

<https://pubs.acs.org/10.1021/acsenergylett.3c01168>

Notes

The authors declare no competing financial interest.

■ ACKNOWLEDGMENTS

D. Chemisana thanks Institutíó Catalana de Recerca i Estudis Avançats (ICREA) for the ICREA Acadèmia award.

■ REFERENCES

- (1) Burger, T.; Sempere, C.; Roy-Layinde, B.; Lenert, A. Present Efficiencies and Future Opportunities in Thermophotovoltaics. *Joule Cell Press* **2020**, *4*, 1660–1680.
- (2) Datas, A.; Vaillon, R. Thermophotovoltaic Energy Conversion. In *Ultra-High Temperature Thermal Energy Storage, Transfer and Conversion*; Elsevier, 2020; pp 285–308. DOI: 10.1016/B978-0-12-819955-8.00011-9.
- (3) Wernsman, B.; Siergiej, R. R.; Link, S. D.; Mahorter, R. G.; Palmisiano, M. N.; Wehrer, R. J.; Schultz, R. W.; Schmuck, G. P.; Messham, R. L.; Murray, S.; Murray, C. S.; Newman, F.; Taylor, D.; DePoy, D. M.; Rahmlow, T. Greater than 20% Radiant Heat Conversion Efficiency of a Thermophotovoltaic Radiator/Module

System Using Reflective Spectral Control. *IEEE Trans. Electron Devices* **2004**, *51* (3), 512–515.

- (4) Woolf, D. N.; Kadlec, E. A.; Bethke, D.; Grine, A. D.; Nogan, J. J.; Cederberg, J. G.; Bruce Burckel, D.; Luk, T. S.; Shaner, E. A.; Hensley, J. M. High-Efficiency Thermophotovoltaic Energy Conversion Enabled by a Metamaterial Selective Emitter. *Optica* **2018**, *5* (2), 213.

- (5) Omair, Z.; Scranton, G.; Pazos-Outón, L. M.; Xiao, T. P.; Steiner, M. A.; Ganapati, V.; Peterson, P. F.; Holzrichter, J.; Atwater, H.; Yablonovitch, E. Ultraefficient Thermophotovoltaic Power Conversion by Band-Edge Spectral Filtering. *Proc. Natl. Acad. Sci. U. S. A.* **2019**, *116* (31), 15356–15361.

- (6) Fan, D.; Burger, T.; McSherry, S.; Lee, B.; Lenert, A.; Forrest, S. R. Near-Perfect Photon Utilization in an Air-Bridge Thermophotovoltaic Cell. *Nature* **2020**, *586*, 237–241.

- (7) Burger, T.; Roy-Layinde, B.; Lentz, R.; Berquist, Z. J.; Forrest, S. R.; Lenert, A. Semitransparent Thermophotovoltaics for Efficient Utilization of Moderate Temperature Thermal Radiation. *Proc. Natl. Acad. Sci. U. S. A.* **2022**, *119* (48), No. e2215977119.

- (8) Datas, A. Bifacial Thermophotovoltaic Energy Conversion. *ACS Photonics* **2023**, *10* (3), 683–690.

- (9) Tervo, E. J.; France, R. M.; Friedman, D. J.; Arulananam, M. K.; King, R. R.; Narayan, T. C.; Luciano, C.; Nizamian, D. P.; Johnson, B. A.; Young, A. R.; Kuritzky, L. Y.; Perl, E. E.; Limpinsel, M.; Kayes, B. M.; Ponec, A. J.; Bierman, D. M.; Briggs, J. A.; Steiner, M. A. Efficient and Scalable GaInAs Thermophotovoltaic Devices. *Joule* **2022**, *6* (11), 2566–2584.

- (10) Datas, A.; Ramos, A.; Martí, A.; del Cañizo, C.; Luque, A. Ultra High Temperature Latent Heat Energy Storage and Thermophotovoltaic Energy Conversion. *Energy* **2016**, *107*, 542–549.

- (11) Amy, C.; Seyf, H. R.; Steiner, M. A.; Friedman, D. J.; Henry, A. Thermal Energy Grid Storage Using Multi-Junction Photovoltaics. *Energy Environ. Sci.* **2019**, *12* (1), 334–343.

- (12) Datas, A.; López-Ceballos, A.; López, E.; Ramos, A.; del Cañizo, C. Latent Heat Thermophotovoltaic Batteries. *Joule* **2022**, *6* (2), 418–443.

- (13) Amy, C.; Pishahang, M.; Kelsall, C.; LaPotin, A.; Brankovic, S.; Yee, S.; Henry, A. Thermal Energy Grid Storage: Liquid Containment and Pumping above 2000 °C. *Appl. Energy* **2022**, *308*, 118081.

- (14) Lee, B.; Lentz, R.; Burger, T.; Roy-Layinde, B.; Lim, J.; Zhu, R. M.; Fan, D.; Lenert, A.; Forrest, S. R. Air-Bridge Si Thermophotovoltaic Cell with High Photon Utilization. *ACS Energy Lett.* **2022**, *7* (7), 2388–2392.

- (15) Schulte, K. L.; France, R. M.; Friedman, D. J.; Lapotin, A. D.; Henry, A.; Steiner, M. A. Inverted Metamorphic AlGaInAs/GaInAs Tandem Thermophotovoltaic Cell Designed for Thermal Energy Grid Storage Application. *J. Appl. Phys.* **2020**, *128* (14), 143103.

- (16) LaPotin, A.; Schulte, K. L.; Steiner, M. A.; Buznitsky, K.; Kelsall, C. C.; Friedman, D. J.; Tervo, E. J.; France, R. M.; Young, M. R.; Rohskopf, A.; Verma, S.; Wang, E. N.; Henry, A. Thermophotovoltaic Efficiency of 40%. *Nature* **2022**, *604* (7905), 287–291.

- (17) Gover, A.; Stella, P. Vertical Multijunction Solar-Cell One-Dimensional Analysis. *IEEE Trans. Electron Devices* **1974**, *21* (6), 351–356.

- (18) Sater, B. L.; Sater, N. D. High Voltage Silicon VMJ Solar Cells for up to 1000 Suns Intensities. In *Conference Record of the IEEE Photovoltaic Specialists Conference*; 2002; pp 1019–1022. DOI: 10.1109/pvsc.2002.1190778.

- (19) Pozner, R.; Segev, G.; Sarfaty, R.; Kribus, A.; Rosenwaks, Y. Vertical Junction Si Cells for Concentrating Photovoltaics. *Prog. Photovoltaics Res. Appl.* **2012**, *20* (2), 197–208.

- (20) Ekstedt, T. W.; Mahan, J. E.; Frank, R. I.; Kaplow, R. Open-Circuit Voltage of Vertical-Junction Photovoltaic Devices at High Intensity. *Appl. Phys. Lett.* **1978**, *33* (5), 422–423.

- (21) Dupré, O.; Vaillon, R.; Green, M. A. Physics of the Temperature Coefficients of Solar Cells. *Sol. Energy Mater. Sol. Cells* **2015**, *140*, 92–100.

(22) Sater, B. L. Vertical Multi-Junction Cells for Thermophotovoltaic Conversion. In *AIP Conference Proceedings*; AIP Publishing, 1995; Vol. 321, pp 165–176. DOI: 10.1063/1.47040.

(23) Piness-Sommer, M.; Braun, A.; Katz, E. A.; Gordon, J. M. Ultra-Compact Combustion-Driven High-Efficiency Thermophotovoltaic Generators. *Sol. Energy Mater. Sol. Cells* **2016**, *157*, 953–959.

(24) Green, M. A.; Dunlop, E. D.; Hohl-Ebinger, J.; Yoshita, M.; Kopidakis, N.; Bothe, K.; Hinken, D.; Rauer, M.; Hao, X. Solar Cell Efficiency Tables (Version 60). *Prog. Photovoltaics Res. Appl.* **2022**, *30* (7), 687–701.

(25) Ponce-Alcántara, S.; Connolly, J. P.; Sánchez, G.; Míguez, J. M.; Hoffmann, V.; Ordás, R. A Statistical Analysis of the Temperature Coefficients of Industrial Silicon Solar Cells. *Energy Procedia* **2014**, *55*, 578–588.

(26) Dupré, O.; Vaillon, R.; Green, M. A. Experimental Assessment of Temperature Coefficient Theories for Silicon Solar Cells. *IEEE J. Photovoltaics* **2016**, *6* (1), 56–60.

(27) MH GoPower. <https://www.mhgopower.com/mhmain.html> (accessed 2023-07-05).

(28) De Izarra, C.; Gitton, J.-M. Calibration and Temperature Profile of a Tungsten Filament Lamp. *Eur. J. Phys.* **2010**, *31* (4), 933–942.

Recommended by ACS

Temperature Coefficients of Perovskite/Silicon Tandem Solar Cells

Maxime Babics, Stefaan De Wolf, *et al.*

JUNE 15, 2023
ACS ENERGY LETTERS

READ 

Optical Simulation-Aided Design and Engineering of Monolithic Perovskite/Silicon Tandem Solar Cells

Yifeng Zhao, Olindo Isabella, *et al.*

MAY 02, 2023
ACS APPLIED ENERGY MATERIALS

READ 

Cost Estimates of Roll-to-Roll Production of Organic Light Emitting Devices for Lighting

Boning Qu, Stephen R. Forrest, *et al.*

MAY 18, 2023
ACS PHOTONICS

READ 

Full-Area Passivating Hole Contact in Silicon Solar Cells Enabled by a TiO_x/Metal Bilayer

Takuya Matsui, Hitoshi Sai, *et al.*

SEPTEMBER 16, 2022
ACS APPLIED ENERGY MATERIALS

READ 

Get More Suggestions >